Available online at www.sciencedirect.com
ScienceDirect
Trans. Nonferrous Met. Soc. China 23(2013) 1375−1381
Transactions of Nonferrous Metals Society of China
www.tnmsc.cn

Preparation and oxidation behavior of a novel CeO_2-modified chromizing coating

Jian-feng SUN, Yue-bo ZHOU, Hai-jun ZHANG

College of Materials Science and Engineering, Heilongjiang Institute of Science and Technology, Harbin 150027, China

Received 16 March 2012; accepted 23 November 2012

Abstract: By using CeO_2 particles instead of part of Al_2O_3 particles as filler, the CeO_2 was successfully entrapped into the outer layer of the chromizing coatings on the as-deposited nanocrystalline (NC) and microcrystalline (MC) Ni films using a conventional pack-cementation method at 800 °C. For comparison, chromizing was also performed under the same condition on MC Ni film using Al_2O_3 as filler without CeO_2 particles. SEM/EDX and TEM results indicate that the refinement of Ni grain and CeO_2 entrapped into the chromizing coatings refine the grain of the chromizing coating. Oxidation at 900 °C indicates that compared with the CeO_2-free chromizing coating, the CeO_2-dispersed chromizing coating exhibits an increased oxidation resistance. For the CeO_2-dispersed chromizing coating, the refinement of Ni grain size significantly decreases the transient-oxidation scaling rate of the chromizing coatings. Together with this, the CeO_2-dispersed chromizing coating formed on NC Ni exhibits a better oxidation resistance.
Key words: chromizing; coating; CeO_2; reactive element effect; oxidation behavior

1 Introduction

Chromium coatings, traditionally manufactured using a conventional pack cementation at temperatures above 1000 °C for durations of 6−10 h, limited by the diffusion and reaction kinetics involved, have been widespread to economically improve high temperature oxidation and corrosion resistance of metals [1−5]. However, such a high temperature treatment inevitably limits the applications of chromizing coatings due to the grain growth of substrate materials, which has a detrimental effect on the mechanical properties of workpieces. Therefore, exploration of novel processing techniques by which chromizing kinetics is greatly enhanced at low temperatures is essential for the widespread application of the chromizing coating. WANG et al [6−8] found that the refinement of grain size using so-called surface mechanical attrition treatment (SMAT) significantly enhanced inward diffusion of Cr at low temperatures, thus influencing the corrosion or oxidation resistance of the chromizing coatings. ZHANG et al [9] found that electrodeposition is another method to produce nanostructured materials, and seems to be appropriate for lowering the chromizing temperature (or shortening the duration) in a practical manner. After adding some rare earth (RE) or RE oxides into the chromizing coatings through codeposition of CeO_2 or Y_2O_3 particles into Ni matrix before chromizing, the oxidation resistance of chromizing coatings could be effectively improved [1−5, 9−11]. The phenomenon was first reported in 1937 [12] and is referred as reactive element effect (REE). Various theories to elucidate the REE have been put forward but are still in dispute [13]. However, these methods not only added their technologic step, but also improved the difficulty in preparation for the modified chromizing coatings. It was reported that during the low activity aluminization, the filler Al_2O_3 particles could be entrapped into the outer layer of aluminide coating [14,15] due to the outer growth of the aluminide coating. By considering this phenomenon, ZHOU et al [16] added some Y_2O_3 microparticles into the outer aluminide coating using the Y_2O_3 microparticles instead of part of Al_2O_3 filler. ZHOU et al [11] found that the outer growth also contributed to the formation of chromizing coating at a low temperature (800 °C). Thus, it is reasonable to add the RE oxides into the outer layer of chromizing coatings using the same

Foundation item: Project (11531319) supported by Scientific Research Fund of Heilongjiang Provincial Education Department, China
Corresponding author: Jian-feng SUN; Tel: +86-13206558225; E-mail: sunwind_0l@163.com
DOI: 10.1016/S1003-6326(13)62606-0

methods. So far, studies on the oxidation of chromizing coating with RE oxides additions by CeO_2 nanoparticles as filler have rare been reported. In this work, by considering the beneficial effect of CeO_2 nanoparticles on the oxidation of chromizing coatings, CeO_2-dispersion low temperature chromized coating on the electrodeposited NC Ni film was produced by pack cementation at 800 °C using the CeO_2 nanoparticles instead of part of Al_2O_3 as filler, and its oxidation performance was reported. To clearly elucidate the effect of the grain size of Ni and CeO_2 on the oxidation performance of the chromizing coatings, preparation and oxidation of two chromizing coatings on MC Ni with or without CeO_2 particle dispersion were also studied under the same condition.

2 Experimental

Samples with dimensions of 15 mm×10 mm×2 mm were cut from an electrolytic nickel plate. They were ground with 800# SiC papers. After ultrasonically cleaning in acetone, they were electrodeposited with a 50 μm-thick Ni film from a nickel sulfate bath. The current density used was 3 A/dm^2, the bath temperature was 35 °C, and the pH was 5.6−6.2. The detailed coating process has been provided elsewhere [11]. MC Ni samples were prepared by annealing the as-deposited NC Ni film at 800 °C in pure Ar atmosphere for 40 min. The NC Ni film and some MC Ni samples were buried in a power-mixture-packed cylindrical steel container and sealed. The chromizing powder mixture was 50%Cr (75 μm)+23.5%Al_2O_3 (75 μm) +23.5%CeO_2 (7 nm, commercial product from NanoScale Materials, Inc., Manhattan)+3%NH_4Cl. The container was then placed in a horizontal quartz tube furnace. The quartz tube was first evacuated and then introduced with pure Ar gas for 10 min before heating up the furnace. The chromization was conducted at 800 °C for 7 h in the pure Ar atmosphere. To clearly elucidate the effect of the grain size of Ni base and CeO_2 on the oxidation performance of the chromizing coatings, some MC Ni samples, were chromized in a homogeneous mixture of 50%Cr+ 47%Al_2O_3+3%NH_4Cl under the same condition. Afterward, the chromized samples were brushed, cleaned in bubbling distilled water for 30 min and finally ultrasonically cleaned in acetone to remove loosely embedded pack particles. The various chromized coatings developed on the MC Ni without CeO_2, MC Ni with CeO_2, and as-deposited NC Ni with CeO_2 are labeled as C1, C2 and C3, respectively.

The oxidation experiments were carried out in air at 900 °C for to 20 h and the mass was weighed after fixing time intervals using a balance with 0.01 mg of sensitivity. Three parallel samples were adopted for acquring average mass change during the thermal exposure. The composition and phases of the various coatings before and after oxidation were investigated using Camscan MX2600FE type scanning electron microscope (SEM) with energy dispersive X-ray analysis (EDX), D/Max−2500 pc type X-ray diffraction (XRD) and TECNAI−20 type transmission electron microscope (TEM). The average chromium concentrations in the surface zone were analyzed using area analysis. Ten replicate tests at different locations were carried out so as to minimize data scattering, and every value was an average of ten measurements. Electroless Ni-plating was plated on the surface of the oxidized specimens to prevent the spallation of the scales for observing cross-sections.

3 Results

3.1 Microstructure

The size of the as-deposited NC Ni film [11] is in a range of 15−60 nm according to the measurement from a few hundred grains selected randomly, which is finer than the grain size of the MC Ni with the mean value of 1 μm (Fig. 1). Both films formed numerous twins. No defects such as pores and cracks were observed.

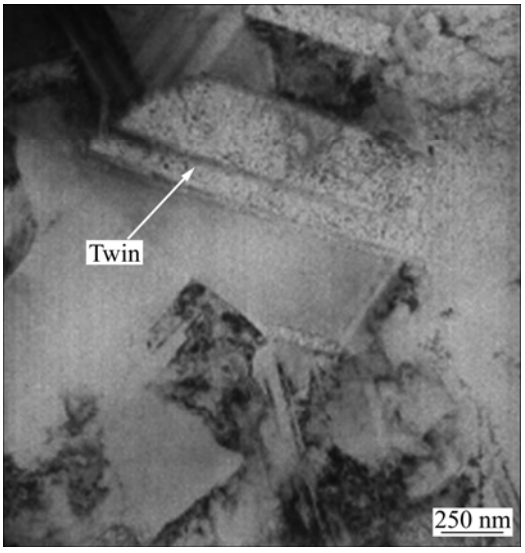

Fig. 1 TEM bright-field image of prepared MC Ni

After pack cementation at 800 °C for 7 h, the chromized layers on various samples were prepared. The average chromium concentrations in the surface zone (<4 μm: the profile depth of electron beam) are close to 40% for C1, 44% for C2 and 57% for C3 by EDX area analysis, as shown in Fig. 2.

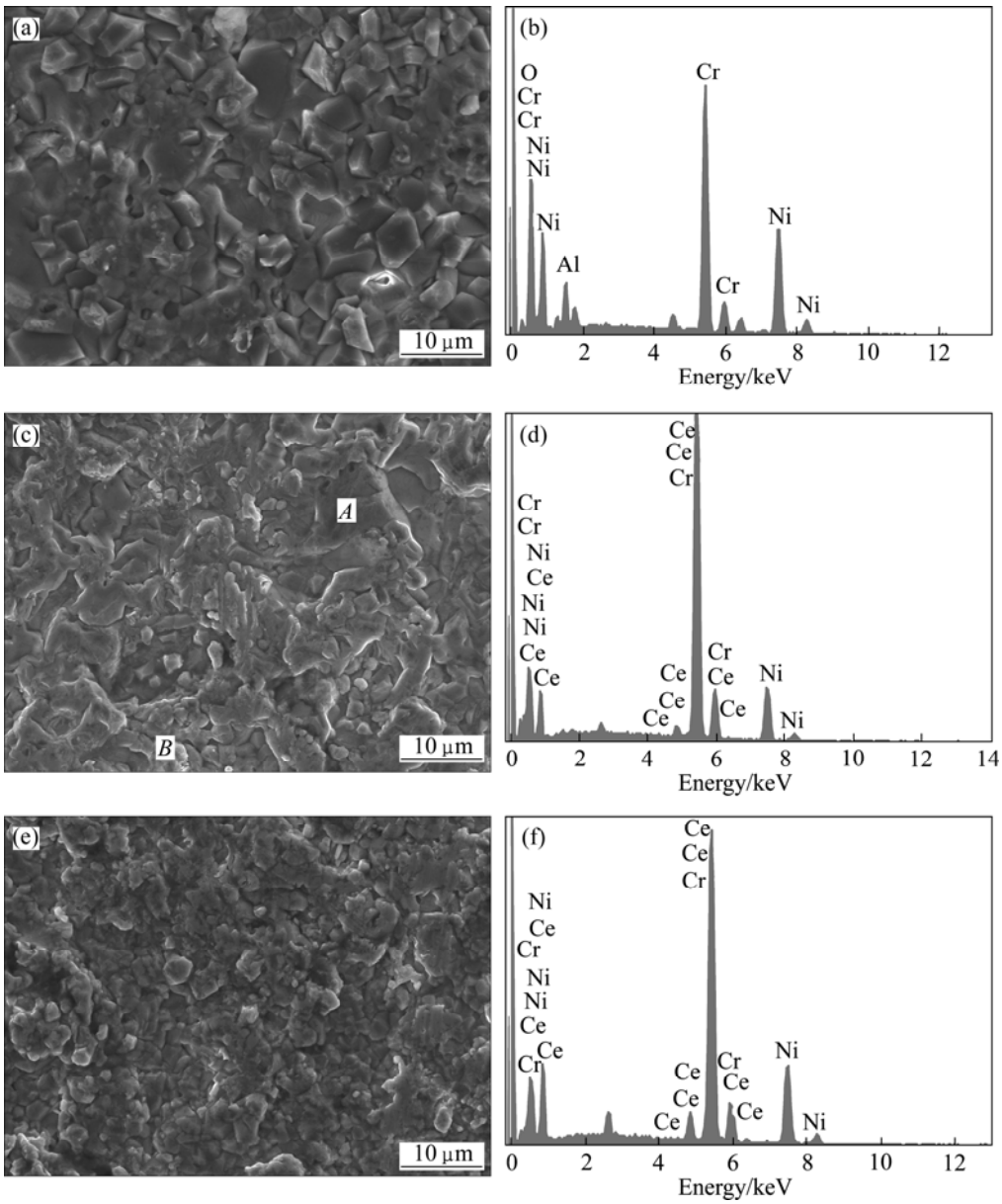

Fig. 2 SEM images (a, c, e) and corresponding EDX (b, d, f) of various chromizing coatings: (a), (b) C1; (c), (d) C2; (e), (f) C3 (CeO_2 particles are entrapped into chromizing coating for C2 and C3)

Figure 2 shows the SEM images and the corresponding EDX of the various chromizing coatings. The appearance of Al and O peaks in Fig. 2(b) would attribute to the loosely embedded Al_2O_3 particles. However, Figs. 2(d) and (f) clearly exhibit that the CeO_2 particles are successfully entrapped into the outer layer of C2 and C3 using CeO_2 particles instead of part of Al_2O_3 as filler. Two distinct morphologies with different grain sizes appear for C2, as seen in Fig. 2(c). The morphology in area *A* is similar to that of C1 with a large grain size. However, the morphology in area *B* with higher Ce contents exhibits a finer grain structure, which is similar to that of C3. The results discussed above suggest that after being entrapped into the chromizing coating, CeO_2 particles significantly retard the grain growth of the chromizing coating, as seen from Figs. 2(a) and (c). Figures 2(c) and (e) show that the refinement of Ni grains before the chromizing process also contributes to the formation of finer grain chromizing coating. Together with this, the finest grain size can be observed for C3, as presented in Fig. 2(e). Previous investigation [16] exhibited that the grains of the chromizing coatings formed on electrodeposited nanocrystalline Ni (15−60 nm) are generally larger than 1200 nm at 800 °C only for 5 h, thus the grains of C1 are also ultrafine-grained and larger than 1200 nm at 800 °C for 7 h. TEM observations show that the grain size of the chromizing coating for C3 near the original coating/gas interface is ultrafine-grained

with the mean size of 1 μm according to the measurement from a few hundred grains selected randomly, as seen in Figs. 3(a) and (b). The corresponding SAED pattern of area *A* in Fig. 3(b) shown in Fig. 3(c) further confirmed the presence of nano-sized CeO_2 particles for C3. It can be seen that near the CeO_2 particles, the grain sizes are finer, indicating that the grain growth of the chromizing coating is retarded by the dispersed CeO_2. The dispersed CeO_2 particles are much larger than the original nanoparticles used, which may be due to the agglomeration or the dissolution and re-precipitation of some CeO_2 nanoparticles during the chromizing process. The grain refinement enhances the diffusion of chromium during pack cementation, leading to a higher Cr content on the coating surface as seen from the EDX analyses.

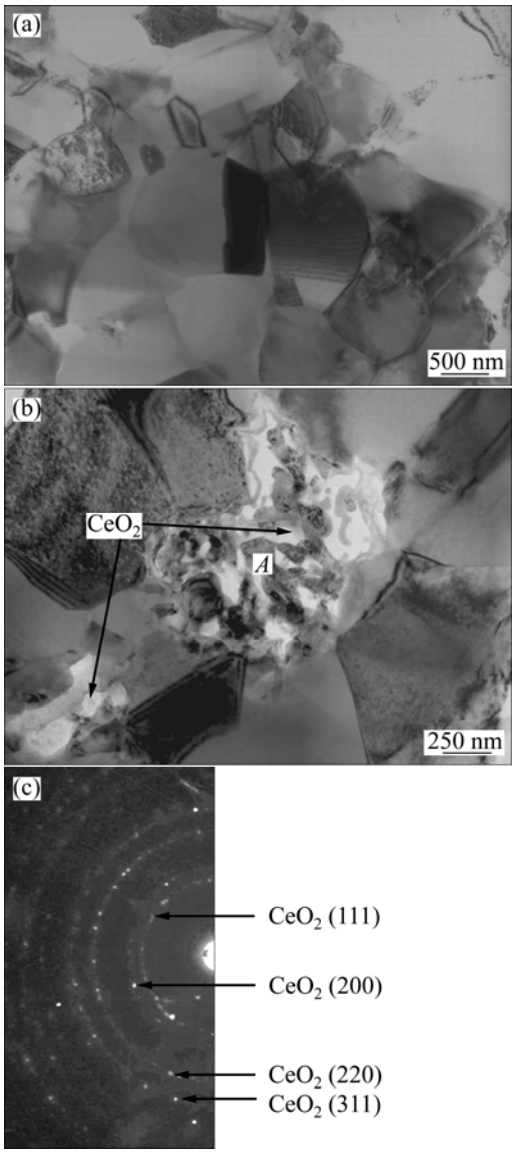

Fig. 3 TEM bright-field images of chromizing coating for C3 at location near original coating/gas interface: (a) Major area without CeO_2 particle; (b) Area with CeO_2 particle; (c) Corresponding SAED pattern of area *A* in (b)

3.2 Oxidation resistance

Figure 4 shows the oxidation curves of the various chromizing coatings in air at 900 °C for 20 h. During the oxidation and cooling, no spallation occurred for the three chromizing coatings. All chromizing coatings obeyed the parabolic rate law to a good approximation. The parabolic rate constant is 2.38×10^{-11} $g^2/(cm^4\cdot s)$ for C1, 7.6×10^{-12} $g^2/(cm^4\cdot s)$ for C2, and 1.22×10^{-12} $g^2/(cm^4\cdot s)$ for C3, as shown in Fig. 3. It is obvious that C2 and C3 exhibit lower scaling rates than C1, particularly in the short transient oxidation stage (the first 2−3 h). In this stage, a continuous, protective chromia scale was expected to thermally grow. After this period, the oxidation rate maintained so extremely low that no significant mass gain occurred for the CeO_2-dispersed chromium coating. However, a significant mass gain occurred for the CeO_2-free chromium coating. The results suggest that the addition of CeO_2 promotes the faster formation of a continuously protective chromia scale. By comparison of the oxidation curves of C2 and C3, it can be seen that the grain refinement of Ni base before chromizing also decreases the transient oxidation rate of the CeO_2-dispersed chromium coating. After the transient oxidation period, both C2 and C3 exhibit a similarly low scaling rate.

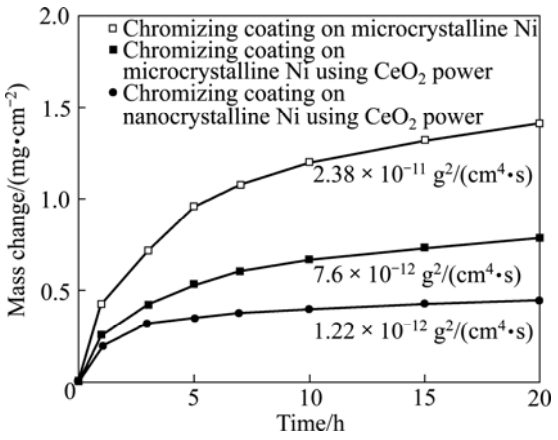

Fig. 4 Oxidation kinetics of chromizing coatings at 900 °C for 20 h

Figure 5 shows that a mixture of NiO, $NiCr_2O_4$ and Cr_2O_3 is formed on C1 but only Cr_2O_3 is formed on C2 and C3. For oxidation of the CeO_2-dispersed chromizing coatings (C2 and C3), a higher intensity peak from the coating substrate appears (see Figs. 5(b) and (c)), suggesting that the chromia scale formed is thinner in this case. In contrast, the chromia formed in the CeO_2-free coating (C3) exhibits a preferential growth on the (202) plane (see Fig. 5(a)). This suggests that the CeO_2 addition significantly suppresses NiO growth, and a purer and denser chromia scale is formed on the

CeO_2-dispersed chromizing coating. This is consistent with the SEM results shown in Figs. 6 and 7.

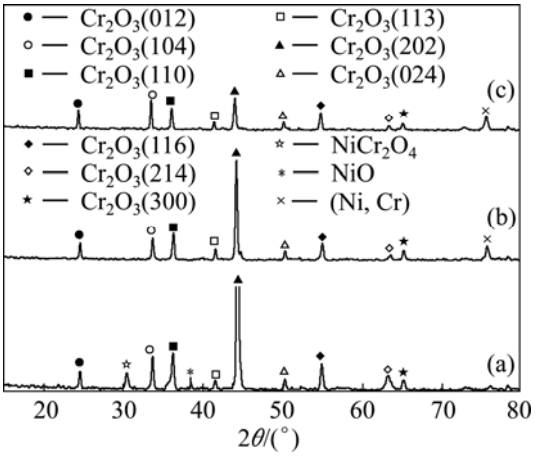

Fig. 5 XRD patterns of different specimens after 20 h oxidation at 900 °C: (a) C1; (b) C2; (c) C3

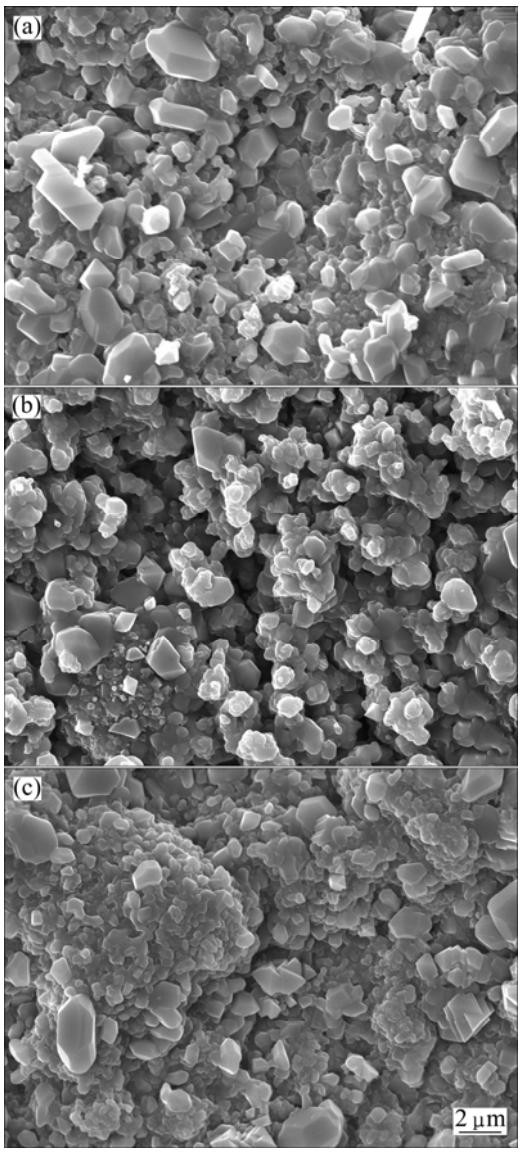

Fig. 6 SEM top-views of scales formed on specimens after 20 h oxidation at 900 °C: (a) C1; (b) C2; (c) C3

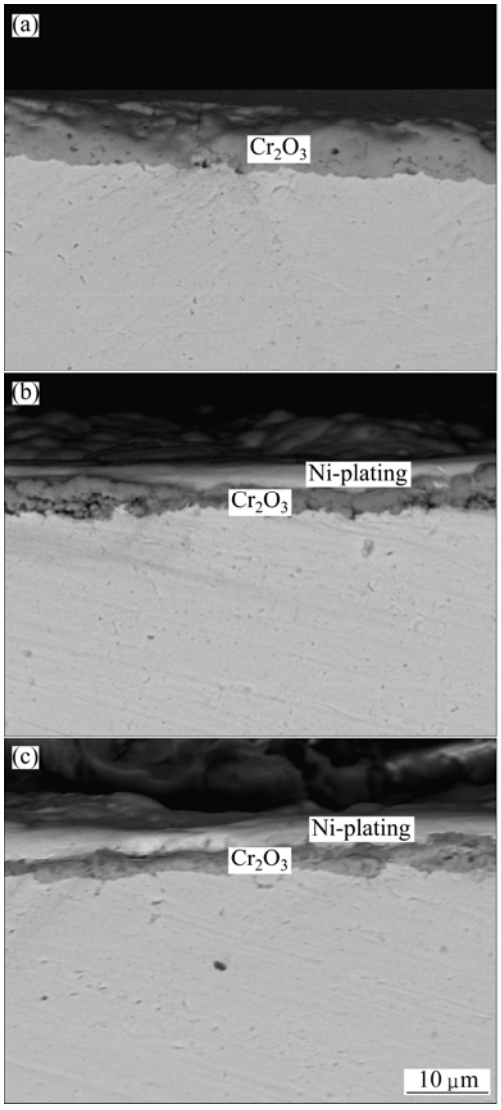

Fig. 7 Backscattered electron images of different specimens after 20 h oxidation at 900 °C: (a) C1; (b) C2; (c) C3

Figure 6 shows the SEM top-views of the scales formed on three chromizing coatings after 20 h exposure at 900 °C. Chromia scales exclusively form on C2 and C3, but minor NiO and $NiCr_2O_4$ form on C1. However, compared with the chromia feature on C2 and C3, the chromia grains on C1 are large. This may be the result of the preferred growth of the oxide on the {202} orient planes as mentioned above. From Figs. 6(b) and (c), it can be found that the chromia scale on C3 is slightly finer than that on C2.

By comparing the corresponding cross-sectional SEM images of the chromia scale on the three chromizing coatings after exposure in air at 900 °C for 20 h as shown in Fig. 7, it can be seen that the oxide scale thickness formed on C2 and C3 is significantly reduced, especially C3, indicating the formation of purer and denser scale on C3. These results suggest that the CeO_2-dispersed chromizing coating exhibits a better

oxidation resistance than the CeO_2-free chromizing coating, which is consistent with the oxidation kinetics in Fig. 4.

4 Discussion

It is generally accepted that for a Ni−Cr alloy with the chromium content over 20%, a chromia layer can thermally form after the establishment of an outer NiO layer at high temperatures [17]. Previous results [11] indicated that even with 50% Cr, a NiO-rich outer layer can still form at 900 °C on the chromizing coatings. In this work, the chromizing coating prepared on MC Ni (C1) exhibits a coarse structure and a low Cr concentration (40% Cr), which could not guarantee the out-ward diffusion flux of chromium far exceeding that of the oxygen atoms from the onset of oxidation. In this case, they cannot exclusively develop a continuous chromia scale. However, the chromizing coatings prepared on MC−Ni (C2) and NC−Ni (C3) have fine structures and high Cr concentrations with surface CeO_2 dispersion, which guarantees the outward diffusion flux of chromium far exceeding that of the oxygen atoms from the onset of oxidation. In this case, they can quickly and exclusively develop a continuous chromia scale at the short transient stage of oxidation. The increased grain boundaries as a result of the refinement of the chromizing coating due to the dispersed CeO_2, together with dispersed CeO_2 particles on the coating surface**,** are both available sites for chromia nucleation at onset of oxidation. The increased chromia nuclei on C2 and C3 with respect to that on C1 shorten the time for their linkage through the oxide lateral growth. The linkage of the chromia nuclei on C2 and C3 is also accelerated because the grain refinement in the finer grained chromizing coatings enhances the diffusion of chromium to the oxidation front, i.e., the oxide/coating interface. Hence, the finer and compact chromia scale was formed on the C2 and C3, especially on C3. In other words, the fine-grain of the CeO_2-dispersed chromized coating enhanced the diffusion of chromium to the oxidation front and consequently accelerated the formation of a continuous chromia layer in a shorter time [1−5, 9−11]. After the establishment of the continuous chromia scale, the scale growth rate should be faster on C2 and C3 than on C1 because the chromia scale on C2 and C3 is finer, especially on C3. The case, however, was not observed from the oxidation kinetics. The reason may be that the chromia scale is incorporated by Ce ions released from the dispersed CeO_2 when they are incorporated into the growing scale. The doped Ce ions segregate to the scale grain boundaries and as a result the dominant grain boundary diffusion of chromium cations for chromia growth will be suppressed [1−5, 9,10].

From above analysis, the lower oxidation rate of CeO_2-dispersed chromizing coating was associated with the effect of CeO_2, which can be summerized as follows. Firstly, CeO_2 entrapped in the chromizing coating led to the formation of a fine-grain chromium-coating, which enhanced the diffusion of chromium to the oxidation front and consequently promoted the formation of chromia layer in a shorter time [1−5, 9,10]. Secondly, the CeO_2 dispersion might release Ce ions, which entered the growing chromia scale [18] and segregated to the scale grain boundaries. In this case, the dominant diffusion of chromium cations during the growth of chromia scale was blocked, leading to a decrease of oxidation. At the same time, the refinement of Ni base led to the formation of a fine-grain chromium-coating structure, which enhanced the diffusion of chromium to the oxidation front and consequently accelerated the healing of the chromia layer at the short transient stage of oxidation.

5 Conclusions

1) Using CeO_2 particles instead of part of Al_2O_3 as filler, the CeO_2 is successfully entrapped into the outer layer of chromizing coatings by a conventional pack-cementation method at 800 °C.

2) The refinement of Ni grain and CeO_2 entrapped into the chromizing coatings refines the grain of the chromizing coating, which obviously decreases the transient-oxidation-scaling rate.

3) The CeO_2-dispersed chromizing coating formed on NC Ni exhibits the best oxidation resistance among the three chromizing coatings due to the formation of purer and denser chromia scale.

References

[1] ZHU L, PENG X, YAN J, WANG F. Oxidation of a novel chromium coating with CeO_2 dispersions [J]. Oxidation of Metals, 2004, 62: 411−426.

[2] YAN J, PENG X, WANG F. Oxidation of a novel CeO_2-dispersion-strengthened chromium coating in simulated coal-combustion gases [J]. Materials Science and Engineering A, 2006, 426: 266−273.

[3] PENG X, YAN J, XU C, WANG F. Oxidation at 900 °C of the chromized coatings on A3 carbon steel with the electrodeposition pretreatment of Ni or Ni−CeO_2 film [J]. Metallurgical and Materials Transactions A, 2008, 39: 119−129.

[4] PENG X, YAN J, DONG Z, XU C, WANG F. Discontinuous oxidation and erosion-oxidation of a CeO_2-dispersion-strengthened chromium coating [J]. Corrosion Science, 2010, 52: 1863−1873.

[5] PENG X, YAN J, ZHENG L AND WANG F. Oxidation of a novel CeO_2-dispersed chromium coating in wet air [J]. Materials and Corrosion, 2011, 62(6): 514−520.

[6] WANG Z B, TAO N R, TONG W P, LU J, LU K. Diffusion of chromium in nanocrystalline iron produced by means of surface mechanical attrition treatment [J]. Acta Materialia, 2003, 51: 4319−4329.

[7] WANG Z B, LU J, LU K. Chromizing behaviors of a low carbon steel processed by means of surface mechanical attrition treatment [J]. Acta Materialia, 2005, 53: 2081−2089.

[8] WANG Z B, LU J, LU K. Wear and corrosion properties of a low carbon steel processed by means of SMAT followed by lower temperature chromizing treatment [J]. Surface and Coatings Technology, 2006, 201: 2796−2801.

[9] ZHANG H, PENG X, ZHAO J, WANG F. Prior electrodeposition of nanocrystalline Ni−CeO_2 film fabricating an oxidation-resistant chromized coating on carbon steels [J]. Electrochemical and Solid-State Letters, 2007, 10(3) C: 12−5.

[10] ZHOU Yue-bo, ZHANG Hai-jun, WANG Yong-dong. Effect of Y_2O_3 on microstructure and oxidation of chromizing coating [J]. Transactions of Nonferrous Metals Society of China, 2008, 18(5): 1122−1127.

[11] ZHOU Y B, CHEN H, ZHANG H, WANG Y. Preparation and Oxidation of an Y_2O_3-dispersed chromizing coating by pack-cementation at 800 °C [J]. Vacuum, 2008, 82: 748−753.

[12] PFEIL B. Improvement in heat-resisting alloys: UK Patent, 459848 [P]. 1937.

[13] MOON D P. Role of reactive elements in alloy protection [J]. Mater Sci Tech, 1989, 5: 754−63.

[14] GOWARD G W, BOONE D H. Mechanisms of formation of diffusion aluminide coatings on nickel-base superalloys [J]. Oxidation of Metals, 1971, 3: 475−495.

[15] XIANG Z D, DATTA P K. Pack cementation process for the formation of refractory metal modified aluminide coatings on nickel-base superalloys [J]. Journal of Materials Science, 2003, 38: 3721−3728.

[16] ZHOU W, ZHAO Y G, LI W, TIAN B, HU S W, QIN Q D. Oxidation behavior of the Y_2O_3-modified aluminide coating on Ti−6Al−4V alloy [J]. Materials Science and Engineering A, 2007, 458: 34−38.

[17] DOUGLASS D L. The oxidation mechanism of dilute Ni−Cr alloys [J]. Corrosion Science, 1968, 8: 665−678.

[18] PINT B A, HOBBS L W. Experimental observations in support of the dynamic segregation theory to explain the reactive-element effect [J]. Oxidation of Metals, 1996, 45: 1−37.

一种新的 CeO_2 改性渗铬涂层的制备与氧化性能

孙俭峰，周月波，张海军

黑龙江科技学院 材料科学与工程学院，哈尔滨 150027

摘 要：利用 CeO_2 颗粒部分替代 Al_2O_3 粉作填充剂对电镀纳米 Ni 和微晶 Ni 进行 800 °C 低温渗铬，将 CeO_2 颗粒渗入涂层的外层，制备了 2 种 CeO_2 改性渗铬涂层。采用相同的工艺在微晶 Ni 上利用不含 CeO_2 的普通渗剂直接渗铬，获得一种不含 CeO_2 粒子的普通渗铬涂层。SEM/EDX 和 TEM 结果表明：基体 Ni 的细化和 CeO_2 颗粒的渗入有利于得到细晶渗铬涂层。在 900 °C 下氧化时，CeO_2 颗粒的渗入明显提高了渗铬涂层的抗氧化性能。对于该 2 种 CeO_2 改性的渗铬涂层，基体 Ni 的纳米化明显降低了涂层在暂态氧化期的氧化速度，使得在纳米 Ni 上制备的 CeO_2 改性渗铬涂层具有更好的抗氧化性能。

关键词：渗铬；涂层；CeO_2；活性元素效应；氧化性能

(Edited by Xiang-qun LI)